

# Fine-Tuning of a Ferrocene|Porphyrin|ITO Redox Cascade for Efficient Sequential Electron Transfer Commenced by an S<sub>2</sub> Photoexcited Special-Pair Mimic

Mitsuhiko Morisue,<sup>†</sup> Dipak Kalita, Noriko Haruta and Yoshiaki Kobuke\*

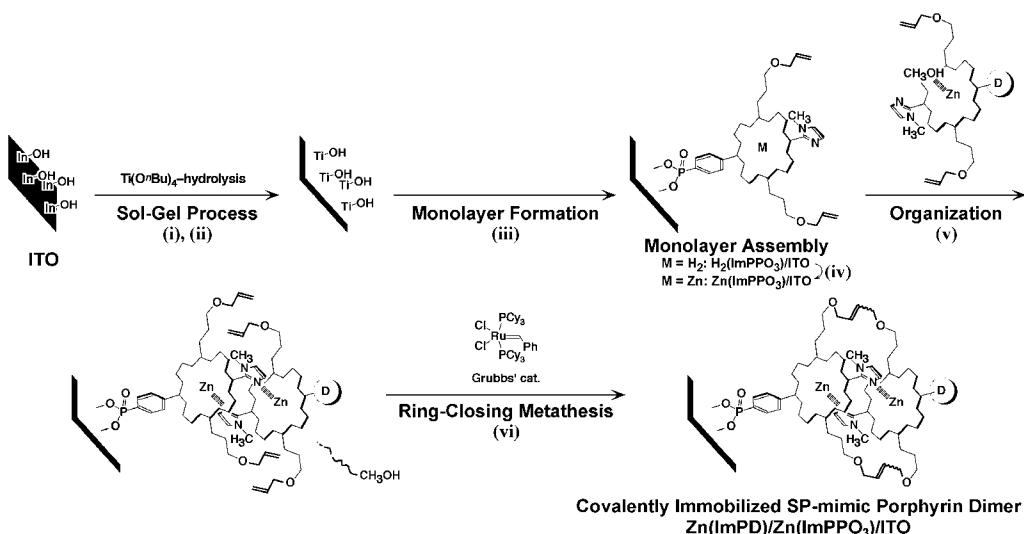
*Graduate School of Materials and Science, Nara Institute of Science and Technology, 8916-5 Takayama, Ikoma, Nara 630-0192, Japan. Fax: (+81)743-72-6119; Tel: (+81)743-72-6110; E-mail: kobuke@ms.naist.jp*

<sup>†</sup>Present Address: Department of Biomolecular Engineering, Graduate School of Science and Technology, Kyoto Institute of Technology, Matsugasaki, Sakyo-ku, Kyoto 606-8585, Japan.

**1. Chemicals and Modification of the ITO surface:** Synthesis of imidazolyl-porphyrins, Zn(ImPPO<sub>3</sub>) and Zn(ImPD)s, were described elsewhere.<sup>S1,S2</sup> Two Zn(ImPD)s spontaneously assemble into the slipped-cofacial dimer in non-coordinating solvent. The dimer structure is controllable by addition/removal of the axial ligand. Therefore, the Zn(ImPD) can be assembled on the Zn(ImPPO<sub>3</sub>)-immobilized ITO electrode surface by dipping in the CH<sub>2</sub>Cl<sub>2</sub> solution of Zn(ImPD) with MeOH as a coordinating soluent and rinsing MeOH with CH<sub>2</sub>Cl<sub>2</sub>. The organized heterodimer, Zn(ImPD)/Zn(ImPPO<sub>3</sub>) was covalently linked by ring-closing olefin metathesis of the allyl side chains catalyzed by Grubbs catalyst. A systematic series of Zn(ImPD)/Zn(ImPPO<sub>3</sub>)/ITO's were thus immobilized as

ferrocene/porphyrin/ITO redox cascade (Scheme S1). The detailed procedure is described in our previous report.<sup>6</sup>

**2. X-ray Photoelectron Spectroscopy (XPS):** The X-ray photoelectron spectra were obtained by an X-ray photoelectron spectrometer (Kratos, AXIS 165) equipped with a monochromatic Al  $K_{\alpha}$  source at 1486.6 eV at a take-off angle of 15°. XPS measurement was carried out for the ITO samples with electrical contact with the spectrometer under external charge neutralization (applied potential: 1.85 V). The residual C(1s) peak at 284.4 eV and the In(3d) at 443.9 eV assignable to In–O bonding was used as internal standard to correct the standard value.



**Scheme S1.** Procedures for preparation of the SP-mimic porphyrin dimer on the ITO electrode surface. (i) A bare ITO electrode was immersed in 100 mM Ti(OnBu)<sub>4</sub> in toluene/ethanol for 3 min. (ii) After rinsing thoroughly with ethanol, the ITO was hydrolysed in water and cleaned by UV-ozone exposure. (iii) The titanium-treated ITO was soaked in H<sub>2</sub>(ImPPO<sub>3</sub>) solution under appropriate conditions. (iv) Zinc(II) was introduced into the porphyrin in the SAM in CHCl<sub>3</sub> containing an aliquot of sat. Zn(OAc)<sub>2</sub> in MeOH at 50 °C for 2 h. (v) The SAM-modified ITO was soaked with 1 mM Zn(ImPD) in CH<sub>2</sub>Cl<sub>2</sub> containing 20 mM MeOH at room temperature for 24 h, and then rinsed with CH<sub>2</sub>Cl<sub>2</sub> to obtain coordination dimer. (vi) The coordination dimer was immobilized covalently by soaking in a dilute solution of Grubbs catalyst at room temperature for 10 min.

Fig S1 compares the survey of XPS spectra and the high resolution spectra for Zn(ImPFc)/Zn(ImPPO<sub>3</sub>)/ITO. We showed the spectral deconvolution analysis of the XPS spectra in the surface sol-gel treatment and the special pair mimic assemblies.<sup>S1</sup>

### 3. Electrochemical and Photocurrent Measurements:

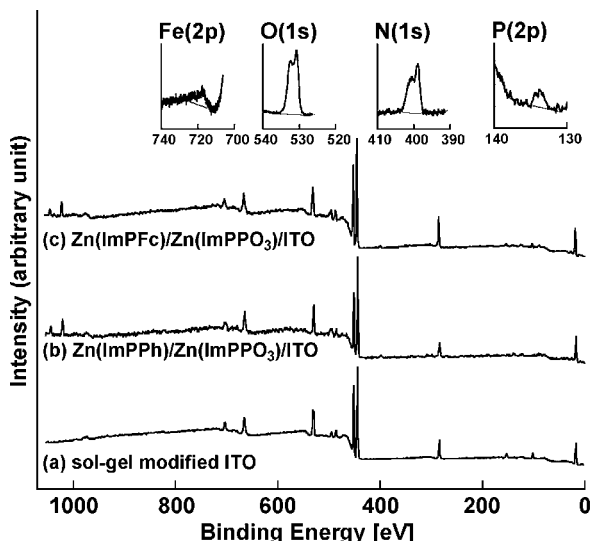


**Fig S1.** Survey of XPS spectra of sol-gel modified ITO (a), Zn(ImPPh)/Zn(ImPPO<sub>3</sub>)/ITO (b), and Zn(ImPFc)/Zn(ImPPO<sub>3</sub>)/ITO (c) observed at a take-off angle of 60° by using monochromatic Al  $K_{\alpha}$ (1486.6 eV). The inset show the magnified spectra of Zn(ImPFc)/Zn(ImPPO<sub>3</sub>)/ITO in the Fe(2p), O(1s), N(1s), and P(2p) region..

electrochemical investigation of the surface-confined porphyrin layers was carried out in the aqueous system under continuous nitrogen flow. The modified ITO working electrodes, mounted at the round cell window (area was 0.28 cm<sup>2</sup>) to be exposed to an electrolyte solution. Platinum wire and Ag/AgCl(sat. KCl) were used as an auxiliary and a reference electrode, respectively. The conventional three-electrode configuration was connected to a potentiostat (BAS, CV-50W). Aqueous 1.0 M NaClO<sub>4</sub> electrolyte was used as the electrolyte solution for CV measurements.

For the photocurrent measurements, the electrolyte solution containing 50 mM hydroquinone (H<sub>2</sub>Q) as a sacrificial electron donor was employed in a phosphate buffer system (Na<sub>2</sub>HPO<sub>4</sub>, KH<sub>2</sub>PO<sub>4</sub>, pH 6.2). The pH effect and further experimental details are described in the previous report.<sup>S1</sup>

The electrochemical cell was placed at a distance of 31 cm from the lamp house in the dark. Current was monitored at potentiostatic conditions during the on/off cycles of light irradiation from a 150-W xenon arc lamp (Hamamatsu Photonics, L2274 light source equipped with a C7535 power supply and a C4251 starter). The monochromatic light was irradiated through a monochromator (Shimadzu, SPG-120S) on the optical cell window. The excitation light was irradiated on the back side of the ITO electrode. Strict control of the experimental conditions provided good reproducibility for all photocurrent properties.

**Cyclic Voltammetry:** Although the Soret band in the absorption and the characteristic peaks in the XPS spectra apparently proved the existence of the porphyrin on the ITO surface, the redox waves were very faint (Fig S2). Introduction of distal ferrocenyl groups

via phenyl-ethenylene linkage (D = PhFc and PhMe<sub>8</sub>Fc) resulted in the incremental oxidation wave of the inner porphyrin layer without appearance of the oxidation wave in the desired region of ferrocenyl terminals. On the other hand, no redox waves were observed in cases of the ferrocenyl terminals directly connected (D = Fc and Me<sub>8</sub>Fc) and connected via saturated bond (D = C<sub>2</sub>Fc, data not shown). The densely stacked porphyrin layer may not be susceptible to show redox processes because of hydrophobicity and decreased permeability of electrolytes.

**Anodic Photocurrent:** Fig S3 represents photocurrent action

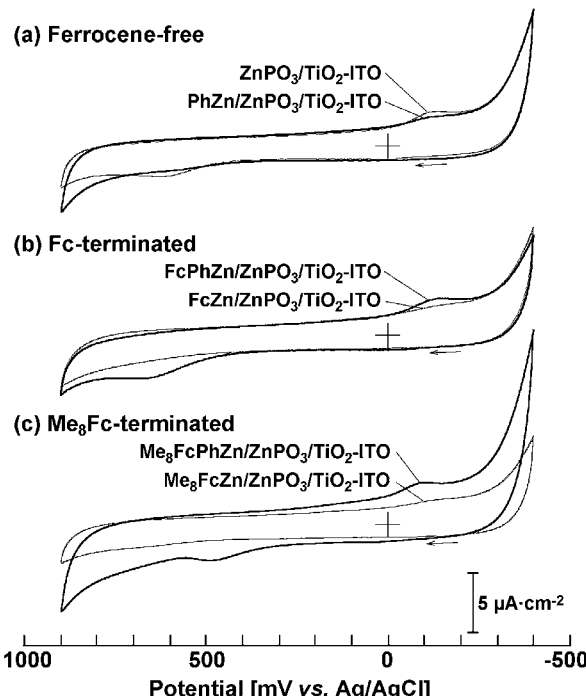


**Fig S2.** Cyclic voltammograms of Zn(ImPD)/Zn(ImPPO<sub>3</sub>)/ITO ITO in aqueous solution with 1.0 M NaClO<sub>4</sub> electrolyte under nitrogen stream at 50 mV·s<sup>-1</sup>.

spectra at 100 mV vs. Ag/AgCl, and the corresponding absorption spectra. The photocurrent response remains the same magnitude over several hours during our experimental operation. The absorption spectra were almost identical irrespective of the ferrocenyl terminal in 350–750 nm region. The direct comparison of the anodic photocurrent observed by excitation at 410 nm is shown in Fig 1. Close coincidence between the photocurrent action spectra and the corresponding absorption spectra indicates clearly that the photoexcitation of the porphyrin on the ITO electrode provides the anodic photocurrent generation. Even though the Q band region appeared in the absorption, the photocurrent obtained by excitation at the Q band region was smaller than that at the Soret band region. This is ascribable to the high efficiency of the charge injection to the ITO conduction band from the S<sub>2</sub> photoexcited state, compared with that to the Fermi level from the S<sub>1</sub> state. The effective injection to the CB level from the higher photoexcited states may also explain the shift of the photocurrent action spectra compared with the corresponding absorption spectra.

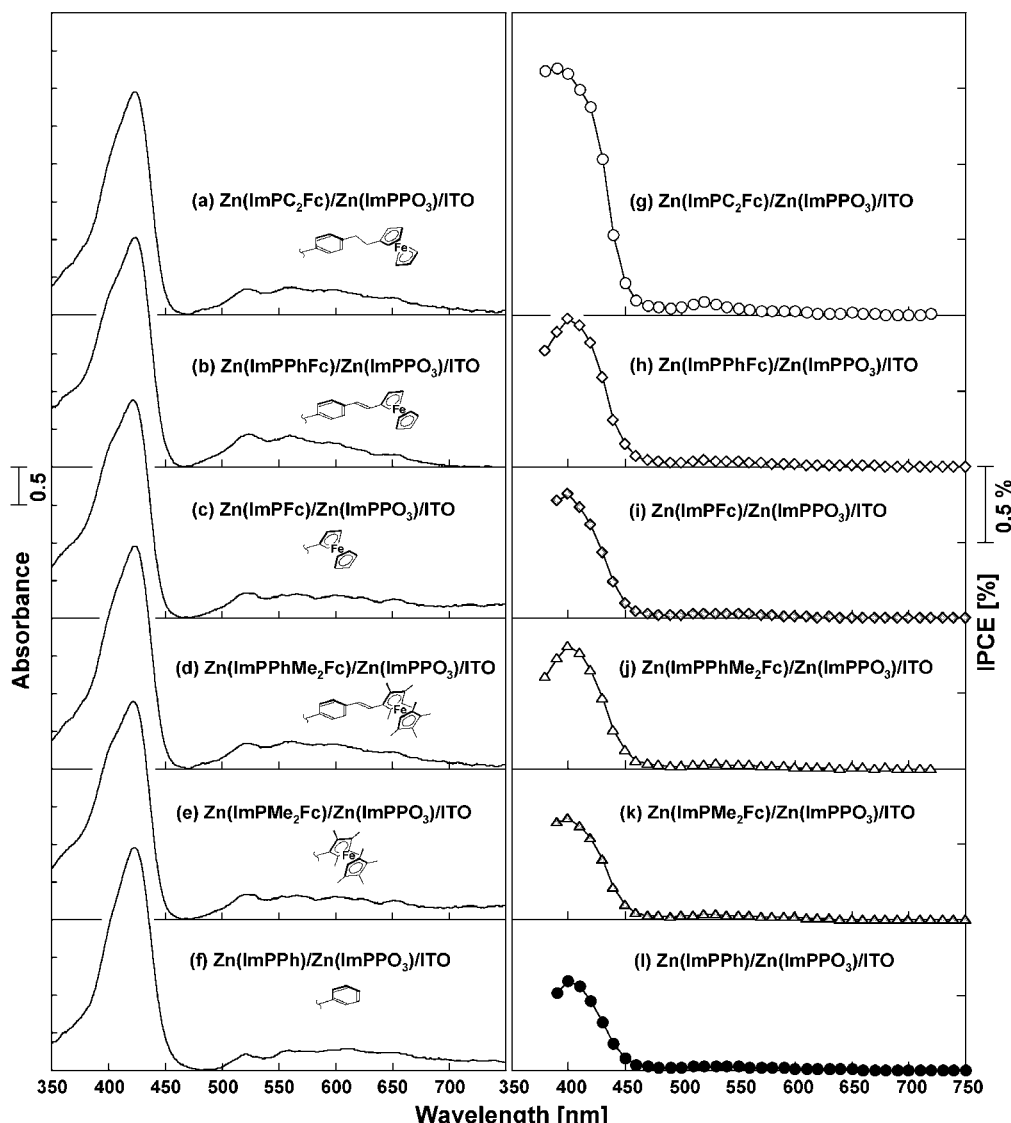


**Fig S3.** Photocurrent action spectra (g-l) and the corresponding absorption spectra (a-f) of  $\text{Zn}(\text{ImPD})/\text{Zn}(\text{ImPPO}_3)/\text{ITO}$  at 100 mV vs. Ag/AgCl. D = C<sub>2</sub>Fc (a and g), PhFc (b and h), Fc (c and i), PhMe<sub>2</sub>Fc (d and j), Me<sub>8</sub>Fc (e and k), and Ph (f and l). The absorption spectrum, shown with correction with background subtraction of the ITO electrode.

## Appendix

The IPCE (incident photon-to-current conversion efficiency) value is determined as follows:

$$\text{IPCE} (\%) = 100 (i/e)/(W\lambda/hc)$$

wherein  $i$ ,  $W$ , and  $\lambda$  are photocurrent density [ $\text{A}\cdot\text{cm}^{-2}$ ], the incident photon flux, and wavelength [nm], respectively. IPCE is an index to evaluate the total profile of the photosensitizing cell at each wavelength. To evaluate the efficiency for conversion of the absorbed photon to current, photocurrent quantum yield  $\Phi$  was employed. The quantum yield  $\Phi$  is defined by the following equation:

$$\Phi (\%) = \text{IPCE}/\text{LHE}$$

wherein LHE is light harvesting efficiency ( $\text{LHE} = 1 - 10^{-A}$ ).

## References

- S1 M. Morisue, N. Haruta, D. Kalita, Y. Kobuke, *Chem. Eur. J.* 2006, **12**, 8123.
- S2 D. Kalita, M. Morisue, Y. Kobuke, *New. J. Chem.* 2006, **30**, 77.